Cellular Signalling 62 (2019) 109356

Contents lists available at ScienceDirect

Cellular Signalling

journal homepage: www.elsevier.com/locate/cellsig

Retinoic acid downregulates thiol antioxidant defences and homologous recombination while promotes A549 cells sensitization to cisplatin

Vitor de Miranda Ramos[a,f,*], Juciano Gasparotto[a,e,f], Fabrício Figueiró[a,b], Amanda de Fraga Dias[a,b], Diana Carolina Rostirolla[a,f], Nauana Somensi[a,f], Helen Tais da Rosa[a,f], Lucas Kich Grun[a,c], Florencia María Barbé-Tuana[c,d], Daniel Pens Gelain[a,f], José Cláudio Fonseca Moreira[a,f]

[a] Postgraduate Program: Biochemistry, Universidade Federal do Rio Grande do Sul (UFRGS), Brazil
[b] Laboratório de Sinalização Purinérgica, Departamento de Bioquímica, Instituto de Ciências Básicas da Saúde, Universidade Federal do Rio Grande do Sul, Porto Alegre, RS, Brazil
[c] Group of Inflammation and Cellular Senescence, School of Sciences, Pontifícia Universidade Católica do Rio Grande do Sul (PUCRS), Brazil
[d] Postgraduate Program in Cellular and Molecular Biology, School of Sciences, Pontifícia Universidade Católica do Rio Grande do Sul (PUCRS), Brazil
[e] Departamento de Civil y Ambiental, Universidad de la Costa, Barranquilla, Atlántico, Colombia
[f] Centro de Estudos em Estresse Oxidativo, Departamento de Bioquímica, Instituto de Ciências Básicas da Saúde, Universidade Federal do Rio Grande do Sul, Porto Alegre, RS, Brazil

ARTICLE INFO

Keywords:
Retinoic acid
Cisplatin
A549 cells
NRF2
Antioxidants systems
Homologous recombination

ABSTRACT

Recent studies have investigated the use of retinoic acid (RA) molecule in combined chemotherapies to cancer cells as an attempt to increase treatment efficiency and circumvent cell resistance. Positive results were obtained in clinical trials from lung cancer patients treated with RA and cisplatin. Meanwhile, the signalling process that results from the interaction of both molecules remains unclear. One of the pathways that RA is able to modulate is the activity of NRF2 transcription factor, which is highly associated with tumour progression and resistance. Therefore, the aim of this work was to investigate molecular mechanism of RA and cisplatin co-treatment in A549 cells, focusing in NRF2 pathway. To this end, we investigated NRF2 and NRF2-target genes expression, cellular redox status, cisplatin-induced apoptosis, autophagy and DNA repair through homologous recombination. RA demonstrated to have an inhibitory effect over NRF2 activation, which regulates the expression of thiol antioxidants enzymes. Moreover, RA increased reactive species production associated with increased oxidation of thiol groups within the cells. The expression of proteins associated with DNA repair through homologous recombination was also suppressed by RA pre-treatment. All combined, these effects appear to create a more sensitive cellular environment to cisplatin treatment, increasing apoptosis frequency. Interestingly, autophagy was also increased by combination therapy, suggesting a resistance mechanism by A549 cells. In conclusion, these results provided new information about molecular mechanisms of RA and cisplatin treatment contributing to chemotherapy optimization.

1. Introduction

Physiologically, retinoic acid (RA) is a signalling molecule derived from vitamin A that participates in biological process such as early organogenesis and tissue remodelling [1]. Because of its primary ability to promote cell cycle arrest and trigger cell differentiation, RA has been considered an inducer of tumour growth suppressors, playing an important role in cancer treatment [2]. More recently, studies have explored the efficiency of RA treatment in combination with other existent chemotherapies as an attempt to increase tumour response and circumvent resistance mechanisms in models of glioma [3], hepatocellular carcinoma [4], and non-small cell lung cancer (NSCLC) [5]. More specifically, RA has been tested in clinical trials combined with cisplatin and paclitaxel, demonstrating promising results in NSCLC patients response [6,7]. Therefore, these results create an urgent necessity to better understand the molecular pathways involved in cancer cell response to combination treatments. In this context, most of RA effects are associated with the activation of subtypes of retinoic acid

* Corresponding author at: Department of Biochemistry, Basic Health Science Institute, University of Rio Grande do Sul, Ramiro Barcelos, 2600 Porto Alegre, RS, Brazil.
E-mail address: 0221536@ufrgs.br (V. de Miranda Ramos).

https://doi.org/10.1016/j.cellsig.2019.109356
Received 6 February 2019; Received in revised form 24 June 2019; Accepted 5 July 2019
Available online 06 July 2019

receptors (RARs), which are a family of nuclear receptors that regulate gene expression [8]. Besides their transcription factor function, these receptors are able to interact with different kinases outside the cell nucleus and regulate several signalling cascades in a very cell-type specific manner [9]. These aforementioned mechanisms are part of the non-genomic effects of RA, which are independent of gene expression modulation and have been shown to contribute significantly to cellular responses.

The transcription factor NRF2 regulates the expression of several enzymes related to antioxidant defences/glutathione metabolism, drug detoxification, and metabolic reprogramming, which makes its activation highly associated with cancer initiation, progression and resistance [10–13]. Additionally, increased evidence has correlated NRF2 activation with cellular process that are targets in cancer therapy, such as DNA repair [14] and autophagy [15]. Therefore, there is a necessity for identifying chemicals that can regulate its activation, suppressing its downstream effects. Normally, NRF2 protein is constantly expressed within the cell and directed to degradation by its inhibitor kelch-like ECH-associated protein 1 (Keap1). In the presence of nucleophile agents, Keap1 activity is impaired and NRF2 is able to translocate to the cell nucleus [16]. Interestingly, RA has been shown to modulate the NRF2 pathway in some types of cancer cells [17,18], but the molecular mechanisms underlying this effect are still poorly understood.

Taking this into account, the aim of this work was to investigate the molecular mechanism by which RA treatment can affect the A549 lung cancer cell line response to cisplatin chemotherapy, focusing mainly on the activity of the transcription factor NRF2. Particularly, we provide information on the effects of RA on NRF2 and NRF2 target gene expression, cellular redox status, cisplatin-induced apoptosis, and DNA repair through homologous recombination (HR). Taken together, these data provide new insight into RA application in cancer treatment, which may contribute to the optimisation of combination therapies.

2. Material and methods

2.1. Chemicals

All-trans retinoic acid (RA), *n*-acetyl-cystein (NAC), cisplatin, 2′,7′-dichlorofluorescin (DCFH-DA), 3-(4,5-dimethyl)-2,5-diphenyl tetrazolium bromide (MTT), sulforhodamine B (SRB), acridine orange (AO) and anti-RAD51 (HPA039310) were purchased from Sigma-Aldrich®. Anti-NQO1 primary antibody (M0716672) and MitoSOX™ Red were purchased from Thermo-Fisher Scientific, USA. Electrophorese reagents were all purchased from Bio-Rad. Anti-NRF2 (M200–3) was purchased from MBL. Anti-β-actin (#3700) and anti-Histone H3 (#4499) were from Cell Signalling Technology.

2.2. Cell culture and treatments

A549 cells (kindly donated by Prof. Claudia Simoes, Universidade Federal de Santa Catarina, Brazil) were grown in culture flasks containing RPMI-1640 (Sigma-Aldrich®) medium supplemented with 10% fetal bovine serum (FBS) and 1× antibiotic/antimycotic (Gibco™). Flasks were maintained inside a humidified incubator at 37 °C with 5% CO_2 atmosphere. When confluence was reached, cells were trypsinized and seeded at culture plates for further experiments. Treatments started 24 h after seeding. All chemicals were previously diluted in culture medium at higher concentrations before added to each well reaching final concentration. Retinoic acid stock solution was dissolved in DMSO and stored at −20 °C protected from light for no longer than two weeks. RA concentration was determined by spectrophotometry read at 351 nm immediately before treatments. *N*-acetyl-cysteine and cisplatin stock solutions were dissolved in PBS and water, respectively, and stored at −20 °C protected from light.

2.3. Sulforhodamine B assay

The percentage of attached live cells was estimated by colorimetric quantification of sulforhodamine B (SRB) stained cells [19]. This method will only quantify the percentage of cells that remained attached to the plate after treatments, and do not consider differences on live cells functioning. After treatments, culture medium was removed, and adhered cells were fixated with 10% trichloroacetic acid (TCA) for 1 h at 4 °C. The precipitated proteins were then stained by 15 min incubation with a 0.4%(w/v) SRB solution dissolved in 1% acetic acid. Excess unbound dye was removed by washing with 1% acetic acid (3-times); stained cells were solubilized in a 10 mM Tris base solution (pH 10.5). Absorbance was quantified using SpectraMAX i3 (Molecular Devices) spectrophotometer set at 515 nm.

2.4. RT-qPCR

Total RNA extracts were obtained by Trizol® reagent (Invitrogen, USA) isolation protocol. Immediately after isolation, total RNA was quantified and used to cDNA synthesis accordingly to High-Capacity cDNA Reverse Transcription Kit (Thermo-Fischer, USA). All reactions were performed by 7300 Real-Time PCR system (Applied Biosystem) and samples were amplified in duplicates using 10 ng of cDNA. Power SYBR™ Green PCR Master Mix (Thermo-Fischer, USA) was used at a final reaction volume of 20 μL per well and specific pair of primers concentration was determined by preceding efficiency tests. All primers sequences had their specificity previously tested by Primer-BLAST tool and were synthetized by Sigma-Aldrich®, Brazil. Relative quantification was obtained by $2^{-\Delta\Delta CT}$ method using GNB2L as housekeeping gene. Primers sequences are described in Table 1.

Table 1
RT-qPCR human primers sequences used in this work.

Gene name	Forward sequence (5′-3′)	Reverse sequence (5′-3′)
NQO1	CCTTGTGATATTCCAGTTCCCC	AGGGTCCTTTGTCATACATGG
GCLC	AAAAGTCCGGTTGGTCCTG	GTTTTCGCATGTTGGCCTC
GCLM	ACTAGAAGTGCAGTTGACATGG	AGGCTGTAAATGCTCCAAGG
GSTP1	TTGGGCTCTATGGGAAGGAC	GGGAGATGTATTTGCAGCGGA
ME1	TGCCTATTGTTTATACTCCCACTG	TTCCATTACAGCCAAGGTCTC
NFE2L2	ACATCCAGTCAGAAACCAGTG	CCGGGAATATCAGGAACAAGTG
TXNRD1	ATATGGCAAGAAGGTGATGGTCC	GGGCTTGTCCTAACAAAGCTG
G6PD	TCTGCCCGAAAACACCTTC	GCATTCATGTGGCTGTTGAG
TALDO1	GCCGAGTATCCACAGAAGTAG	GATCCCAGCTTCCTTGTAGAG
TKT	ATCGAGTGCTACATTGCTGAG	CATGCGAATCTGGTCAAAGG
RAD51	AGTGGCTGAGAGGTATGGTC	TGTTCTGTAAAGGGCGGTG
BRCA2	TTCATGGAGCAGAACTGGTG	ATAAGGGCAGAGGAAAAGGTC
GNB2L	GAGTGTGGCCTTCTCCTCTG	GCTTGCAGTTAGCCAGGTTC

2.5. Nuclear extraction

Nuclear protein extracts isolation was performed as previously described [20]. After isolation, protein content was determined by Pierce™ BCA Protein Assay Kit (Thermo-Fisher) and samples were prepared for western blot analyses.

2.6. Immunoblotting

A549 cells protein lysate was prepared in 2× laemli-sample buffer containing 10% of 2-mercaptoethanol. Equal amounts of protein were electrophoresed using self-prepared 10% SDS-PAGE and transferred onto nitrocellulose membranes (Hybond-ECL, GE Healthcare Lifesciences) using the Trans-blot® SD transfer cell (Bio-Rad). Membranes were then incubated in Tris-buffered saline Tween-20 [TBS-T; 20 mM Tris– HCl, pH 7.5, 137 mM NaCl, 0.05% (v/v) Tween 20] containing 5% (w/v) BSA for 1 h at room temperature. Primary antibodies were diluted (1:1000) in TBS-T with 5% dissolved BSA and incubated overnight at 4 °C. Afterwards, membranes were washed and incubated for 2 h at room temperature with specie-specific HRP-conjugated secondary antibodies (1:3000 dilution in TBS-T). The bands were detected using a CCD camera (GE ImageQuant LAS 4000) by adding SuperSignal® West Pico chemiluminescent substrate (Thermo Scientific). Densitometry was quantified by ImageJ software.

2.7. Intracellular reactive species production (DCF assay)

Intracellular reactive species (RS) production was detected using the 2′,7′- dichlorofluorescin (DCFH-DA, Sigma) as described [21]. DCFH-DA stock solution was dissolved in DMSO stored at −20 °C protected from light. Before cells were treated, DCFH-DA was diluted to 100 μM in 10% FBS supplemented medium solution and added to culture plates. Cells were incubated at 37 °C, with 5% CO_2, and protected from light exposure for 1 h. After DCFH internalization, the medium was replaced by fresh medium solution and treatments were initiated. When internalized, RS cause DCFH oxidation and it becomes a fluorophore (DCF), which was monitored using a SpectraMAX i3 (Molecular Devices) fluorescence plate reader (Ex/Em = 485/532 nm). Results were expressed in relative fluorescence units (RFU). Reactive species production rate was obtained by calculating the Δ of individual hours ($RFU_{hour\ x} - RFU_{hour\ x-1}$).

2.8. Mitochondrial superoxide indicator (MitoSOX™ Red)

To access mitochondrial superoxide production, live cells were stained with MitoSOX™ Red probe. Stock solution was dissolved in 13 μL of DMSO reaching the concentration of 5 mM accordingly to the manufacture. By the end of cells exposure to treatments, MitoSOX™ Red probe was diluted in fresh culture medium at a concentration of 20 μM and then added to the wells reaching final concentration of 2 μM. The incubation proceeded for 30 min before culture medium was removed and cells were washed with 1× PBS. At this point, cells were fixed for 10 min with 4% paraformaldehyde and washed one more time with 1× PBS. Equal volumes of PBS were added to the cells and images were taken on Microscopy EVOS® FL Auto Imaging System (AMAFD1000 - Thermo Fisher Scientific; MA, USA).

2.9. Sulfhydryl groups content

Total reduced thiol (SH) content was determined as an estimation of overall intracellular redox status [22]. First, cells extracts were prepared in phosphate buffer and clarified by centrifugation. Protein content was determined by Pierce™ BCA Protein Assay Kit (Thermo-Fisher) and all samples were diluted to equal protein concentrations. Later, samples were mixed in a slightly alkaline buffer with 10 mM of 5,5-dithiobis-2-nitrobenzoic acid (DTNB) dissolved in ethanol. System was incubated for 1 h at room temperature allowing DTNB to react with sulfhydryl groups generating a yellowish coloration. Therefore, absorbance was determined at 412 nm and results were expressed as μmol SH/ mg of protein.

2.10. Cell cycle

First, cells were trypsinized, centrifuged and washed with 1× cold PBS. Then, cell pellet was suspended in 500 μL of permeabilization buffer (10 mM PBS, 0.1% v/v IGEPAL, 1 mg/mL spermine, 50 μg/mL RNAse, and 4 μg/mL PI, pH 7.4). Cells were incubated for 10 min before PI fluorescence was determined by FACSCalibur™ cytometer. DNA content and cell cycle analyses were performed by FLOWJO® software.

2.11. Intracellular labelling of phospho-γH2AX

A549 cells were pre-treated with RA 20 μM for 48 h before cisplatin (10 μg/mL) was added for 16 h. Cells were trypsinized, washed with 1× cold PBS and centrifuged at 1500 rpm for 5 min. Each sample was resuspended in 250 μL of BD Cytofix™ Fixation Buffer (Cat: 554655) and incubated for 20 min at 4 °C. Afterwards, 400 μL of 1× BD Perm/Wash™ Buffer (Cat: 51-2091KZ) was added. Cells were then centrifuged at 1500 rpm for 5 min and supernatant was removed. Next, 800 μL of 1× BD Perm/Wash™ Buffer (Cat: 51-2091KZ) was added, followed by a new centrifugation at 1500 rpm for 5 min. Supernatant was removed and tubes were vortexed in order to detach cells from the bottom. Slowly, 500 μL of BD Phosflow™ Perm Buffer III (Cat: 558050) was added to each sample while tubes were being shaken. Cells were then incubated for 30 min at 4 °C for proper permeabilization. Samples were then washed two times with cold FACs Buffer (1× filtered PBS + 2% FBS). Cells were resuspended in 50 μL of FACs Buffer and 3 μL of PE Mouse Anti-H2AX (pS139) (Cat: 562377) was added to each sample (except for negative control). Samples were incubated for 30 min at room temperature and protected from light exposure. Afterwards, a wash was performed by adding 1 mL of FACs Buffer and centrifuging tubes. Cells were resuspended in 250 μL of FACs Buffer and antibody labelling was quantified by fluorescence measurement at BD Accuri™ C6, BD Biosciences Flow Cytometer.

2.12. MTT assay

A549 cells viability was assessed by the MTT assay. This method is based on the ability of viable cells to reduce MTT and form a purple formazan product. Therefore, this method considers the number of remaining cells attached to the plate and its functioning. Immediately after treatments, MTT solution prepared in culture medium was added to the cells at a final concentration of 0.5 mg/mL. The cells were incubated for 45 min at 37 °C in a humidified 5% CO_2 atmosphere. The medium was then removed and 200 μL of DMSO was added to each well of 96-well plate. Samples were homogenized by up-and-down pipetting, and optical density of each well was measured at 560 nm (test) and 630 nm.

2.13. LDH activity assay

The leakage of lactate dehydrogenase into culture medium was assessed as a measure of detached cells and losses cell membrane integrity, typically of cultured dead cells. LDH activity was determined by quantifying NADH decay through the conversion of pyruvate in lactate using a commercial kit (Labtest® Brazil). NADH absorbance was obtained by SpectraMAX i3 (Molecular Devices) spectrophotometer set at 340 nm.

2.14. Annexin-V/PI staining

The FITC-Annexin V/PI Detection Kit I (BD Pharmingen™) was used

to evaluate the percentage of apoptotic/necrotic cells. After treatments, culture medium was removed, cells were trypsinized and then washed with cold PBS. Next, cells were suspended in 100 µL of 1× Annexin Binding Buffer (ABB) containing FITC-labelled Annexin and Propidium Iodide (kit provided). After 15 min incubation, 400 µL of ABB was added to each sample and analysed by BD FACSCalibur™ cytometer at FL1-H (FITC) and FL3-H (PI) channels. Proper staining controls were used to set the cytometer. Viable (annexin-/PI-), early apoptotic (annexin + /PI-), late apoptotic (annexin + /PI +) and necrotic (annexin-/PI +) cells were assigned and quantified using FLOWJO® software.

2.15. Acridine orange staining

To access the presence of autophagosomes acidification, cells were stained with acridine orange (AO) which, at low pH environments, changes its fluorescence emission from green to red. After treatments, culture medium was collected and cells trypsinized. At this point, cells were pelleted by centrifugation and washed once with cold PBS to remove remaining culture medium. Cells were then suspended in 300 µL of 1× PBS containing 1 µg/mL of AO followed by 15 min incubation at room temperature. Red/green (FL3-H/FL1-H) fluorescence was measured by BD FACSCalibur™ cytometer. Percentage of autophagy positive cells was calculated using FLOWJO® software as described [23].

2.16. Statistical analysis

Statistical analyses were performed using GraphPad Prism 7 software. Student's *t*-test was applied to compare two groups (one parameter). Two-way ANOVA followed by Bonferroni or Tukey (specified in figures captions) post hoc test was applied to compare multiple groups (two parameters). $p < .05$ was considered statistically significant. Results are expressed by means ± SD. * = $p < .05$; ** = $p < .01$; *** = $p < .001$. All experiments were performed at least three individual times.

3. Results

3.1. Retinoic acid decreases A549 cells proliferation and downregulates NRF2 activity

First, the effects of RA on the growth and viability of A549 cells were tested in order to determine a proper dosage and exposure time. Therefore, cells were treated with 10, 20, or 40 µM of RA for 24, 48, or 72 h. The percentage of attached cells was quantified by the SRB assay (Fig. 1A) simultaneously to the measurement of LDH activity in the culture medium as an indication of dead cells (Fig. 1B). After 24 h of treatment, no significant change in cell growth (SRB assay) was observed in the presence of RA when compared to DMSO (all *p values* > .999; Fig. 1A 24 h). After 48 h, 10 µM RA induced a difference of 0.15-fold when compared to DMSO, but this was not statistically significant (*p value* = .2021). RA at 20 and 40 µM induced a significant difference of 0.21-fold (*p value* = .0390) and 0.64-fold (*p value* < .0001) (Fig. 1A 48 h). After 72 h, all studied doses presented a significant decrease in the percentage of A549 cells, with a mean difference of 0.7–3, 1.23-, and 2.23-fold (*p values* < .0001) for 10, 20 and 40 µM, respectively, when compared to DMSO (Fig. 1A 72 h). When LDH activity was analysed, no significant increase was detected by any of RA doses at these time points (Fig. 1B), indicating that RA treatment did not lead to A549 cell death at the studied concentrations. Therefore, we conclude from the results in Fig. 1A that the reduced percentage of viable cells in the RA-treated groups was due to an antiproliferative effect of RA rather than a cytotoxic effect. Fig. 1C shows representative phase contrast images showing the reduced number of A549 cells with RA treatment compared to DMSO at 72 h. As the focus of our study was to investigate the signalling effects of RA, we decided to proceed with further experiments at an intermediate dose of 20 µM, where we could observe significant effects on A549 cells without the risk of any cytotoxic interference.

To assess the effects of RA on NRF2 activity, RT-qPCR was conducted for some NRF2 target genes. The expression of genes related to thiol antioxidant systems (*GCLC, GCLM, TXNRD1*), detoxification enzymes (*NQO1, GSTP1*), and metabolic reprogramming/NADPH generation (*G6PD, TALDO1, TKT, ME1*) was quantified after 24 and 48 h of RA exposure. After 24 h of treatment, four of the ten evaluated genes showed significantly decreased expression in the RA group as compared to the DMSO group (*NQO1* 0.26-fold, *GCLCI* 0.32-fold, *GCLM* 0.24-fold, and *GSTP1* 0.15-fold; Fig. 1D-24 h). Moreover, all analysed genes, including NRF2 itself (*NFE2L2*), showed significantly decreased expression after 48 h of RA treatment compared to DMSO (*NQO1* 0.43-fold, *GCLM* 0.37-fold, *GCLC* 0.57-fold, *TXNRD1* 0.35-fold, *GSTP1* 0.35-fold, *G6PD* 0.56-fold, *TALDO1* 0.28-fold, *TKT* 0.46-fold, *ME1* 0.56-fold, *NFE2L2* 0.38-fold; Fig. 1D 48 h), indicating an inhibitory effect of RA on NRF2 activity in A549 cells. Finally, the presence of NRF2 in the cell nucleus was investigated by western blot of the nuclear fraction as an indication of its activity. RA treatment decreased nuclear NRF2 protein in A549 cells after 48 h, as shown by Fig. 1E. Taken together, these results demonstrate that RA, at a concentration of 20 µM, is able to inhibit NRF2 protein expression after 48 h as well as downregulate NRF2 target genes in A549 cells.

3.2. Retinoic acid alters the cellular redox environment

Knowing that RA can promote intracellular reactive species (RS) production in different cell types [20,24], and that NRF2 is a major regulator of cell redox status [25], we decided to investigate the effects of RA on the cellular redox environment. To this end, intracellular RS production was indirectly measured by DCFH oxidation. DCF fluorescence data is shown as raw fluorescence values in Fig. 2A and as delta values ($RFU_{hour\ x} - RFU_{hour\ x-1}$) as indicative of the RS production rate in Fig. 2B. In the first hour, RA treatment significantly increased the reactive species production rate in a dose-dependent manner (Fig. 2A and B 1 h), which remained significant in the following hour (Fig. 2B 2 h). For six hours of RA exposure, no significant change in the RS production rate was observed as compared to DMSO (Fig. 2B 6 h). Next, we investigated mitochondrial superoxide (O_2-) generation. Cells treated with RA for 3 h showed greater O_2– production than cells treated with DMSO (Fig. 2C 3 h). In contrast, when the end point was extended to 6 h, this difference was significantly decreased between the groups (Fig. 2C 6 h), corroborating the DCF assay results. Thus, it is evident that RA treatment induced a peak of RS production in the initial hours within cells, then started to decrease its rate in the following hours, approaching control levels by 6 h.

Considering the increase in RS production following RA treatment (Fig. 2A, B, C) and RA-induced downregulation of thiol antioxidant enzyme expression (*GCLC*, *GCLM* and *TXNRD1*; Fig. 1D), we quantified total sulfhydryl groups (R-SH) in A549 cells treated with RA after 24 and 48 h. As a result, we found a lower concentration of reduced sulfhydryl groups in RA treated cells compared to DMSO (Fig. 2D), indicating an oxidised cellular state.

3.3. Retinoic acid affects cisplatin-induced homologous recombination proteins expression, cell cycle arrest, but not phosphorylation of γ-H2AX

Knowing that DNA cross-linking is one of the major cytotoxic effects of cisplatin [26], we investigated the effects of RA pre-treatment on DNA damage signalling in A549 cells induced by cisplatin. Considering the previous results, A549 cells were pre-treated with RA (20 µM) for 48 h before cisplatin (10 µg/mL) addition in further experiments. First, we evaluated the immunocontent of phopho-γ-H2AX protein as an indication of double-strand DNA breaks (Fig. 3A). A549 cells were pre-treated with RA for 48 h and then treated with cisplatin for an additional 16 h before the antibody labelling protocol was performed. The

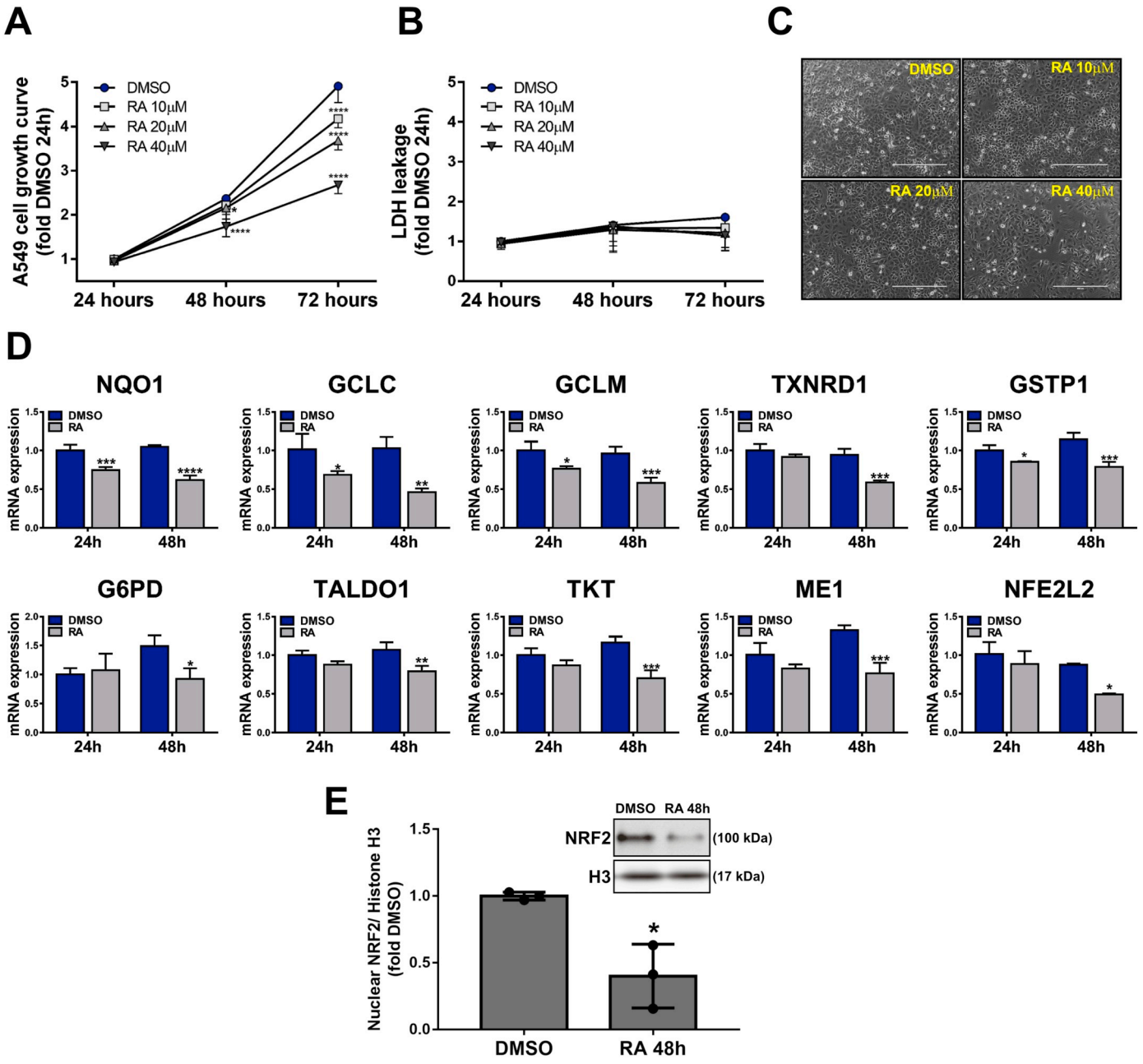

Fig. 1. Retinoic acid decreases A549 cells proliferation and downregulates NRF2 activity. (A) A549 cells growth curve measured by sulforhodamine B Assay and (B) LDH activity measured in culture medium as indicative of dead cells 24, 48 and 72 h after retinoic acid (RA) treatment (10, 20 and 40 μM). Results are expressed in fold change relative to DMSO-24 h group. Two-way ANOVA followed by Bonferroni post hoc test was conducted comparing each RA concentration to DMSO control at its relative time point. (C) Phase contrast and representative images of A549 cells treated with DMSO (vehicle control), 10, 20 and 40 μM of RA after 72 h. (D) mRNA levels of NRF2-target genes measured by RT-qPCR 24 and 48 h after 20 μM RA treatment. Results are expressed in mRNA fold-change relative to DMSO treatment at 24 h. Gene's names are expressed in each graph title. Relative quantification was obtained by $2 - \Delta\Delta CT$ method using GNB2L as housekeeping gene. Two-way ANOVA followed by Bonferroni post hoc test was conducted comparing RA treatment to DMSO at its relative time point group. (E) Nuclear NRF2 immunocontent relative to Histone H3 protein 48 h after RA treatment (20 μM) obtained by Western Blot images. Result is expressed in fold-change relative to DMSO group. Representative Western Blot image is shown in the up-right corner. Student's *t*-test was applied to evaluate statistical significance. Graphs are shown by means ± SD. *, **, *** and **** means $p < .05$, $p < .01$, $p < .001$ and $p < .0001$, respectively.

results in Fig. 3A(I) are shown as median fluorescence intensity (MFI), Fig. 3A(II) represents the percentage of labelled positively marked cells in the population and Fig. 3A(III) is a representative overlay histogram of fluorescence intensity (x-axis) against cell number (y-axis). RA alone did not lead to a significant change in the phopho-γ-H2AX immunocontent compared to DMSO (Fig. 3A(I), RA-control). Cisplatin alone increased the phopho-γ-H2AX immunocontent from 19.85 MFI (Fig. 3A(I), DMSO-control) to 52.26 MFI (Fig. 3A(I), DMSO-cisplatin), indicating DNA damage. RA pre-treatment had no significant effect on cisplatin-induced DNA damage indicated by phopho-γ-H2AX immunocontent, with an average MFI of 52.35 (Fig. 3A(I), RA control).

Homologous recombination is the main pathway that repairs DNA double-strand breaks and is also responsible for cisplatin resistance in tumour cells [27,28]. Previous reports have shown that NRF2 can regulate RAD51 (an HR signalling protein) expression [14]. Therefore, the mRNA content of RAD51 and one of its regulator proteins, BRCA2, was quantified 24 h after cisplatin treatment. NQO1 expression was measured simultaneously as an indication of NRF2 activity. RA was

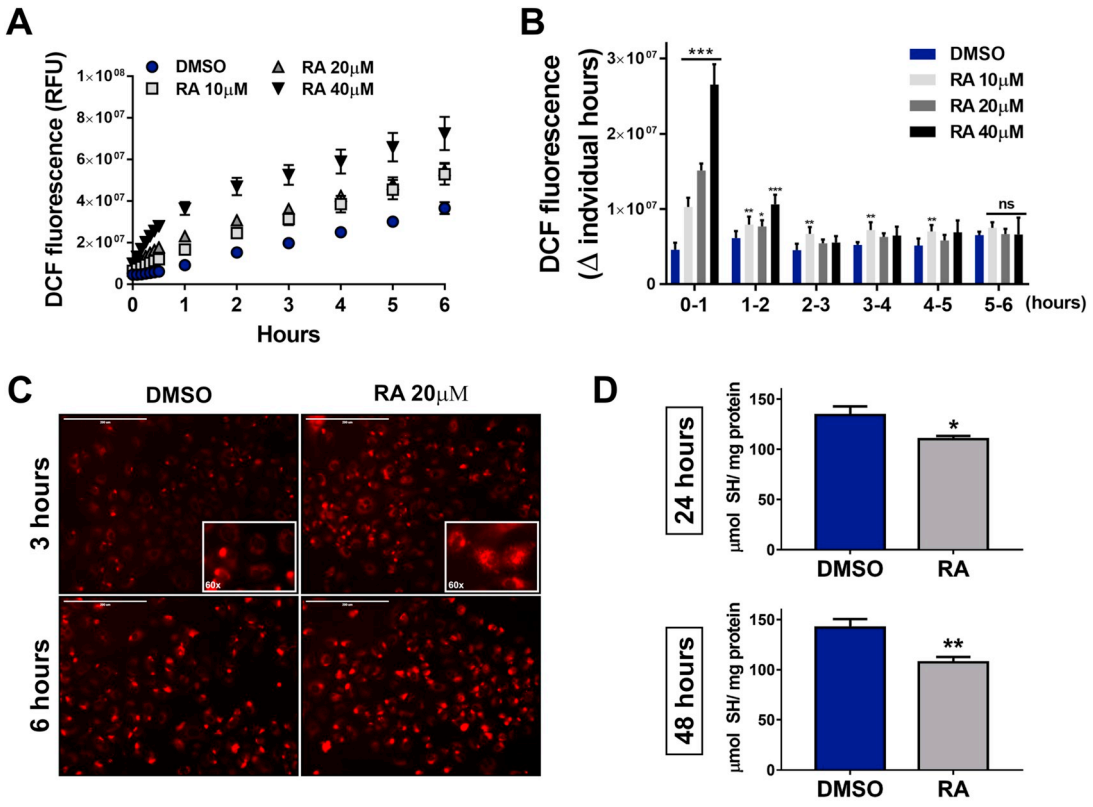

Fig. 2. Retinoic acid alters cellular redox environment. (A) Time curve (*x* axis) of DCF fluorescence expressed in relative fluorescence unit (RFU) (*y* axis), indicating reactive species formation in A549 cells after RA treatment with 10, 20 and 40 μM. (B) Reactive species production rate ($RFU_{hour\ x} - RFU_{hour\ x-1}$) in A549 cells treated with increasing doses of retinoic acid (RA). This graph was obtained from data of graph A and represents the amount of oxidised DCF generated in each individual hour. Two-way ANOVA followed by Tukey's post hoc test was conducted comparing RA concentrations to DMSO treatment within each time group. (C) Representative fluorescent images indicating superoxide generation assessed by MitoSOX™ Red probe after 3 and 6 h of RA treatment. (D) Total sulfhydryl groups content of A549 cells treated for 24 and 48 h with DMSO or RA 20 μM. Results expressed in μmol of SH/ mg of protein. Student's t-test was applied to evaluate statistical significance. Graphs are shown by means ± SD. *, **, *** and **** means $p < .05$, $p < .01$, $p < .001$ and $p < .0001$, respectively. (For interpretation of the references to colour in this figure legend, the reader is referred to the web version of this article.)

able to significantly reduce the expression of the RAD51 and BRCA2 genes in control and cisplatin-treated cells (Fig. 3B control and cisplatin groups). The western blot results also show that the RAD51 immunocontent was decreased with RA treatment (Fig. 3C). The NQO1 mRNA and protein immunocontent were also downregulated by RA, as shown in Fig. 3B and C, indicating that NRF2 downregulation remains even after cisplatin treatment.

Finally, we analysed cell cycle progression by quantifying total propidium iodide (PI) stained DNA by flow cytometry, since it is known that cell cycle progression has a crucial role in the cell response to DNA damage [29]. RA alone decreased the percentage of S-phase cells, although this change was not statistically significant (*p value* 0.056; Fig. 3D). Further, cisplatin treatment induced major arrest of the cell cycle in the S-phase, reducing the percentage of cells in the G0/G1-phase (*p value* 0.004; Fig. 3D). Curiously, when cells were pre-treated with RA, the percentage of arrested cells in the S-phase was significantly lower than with cisplatin alone (*p value* 0.003), leading to an apparent increase in cells in the G0/G1-phase (*p value* 0.132) (Fig. 3D). Therefore, these results reveal that RA pre-treatment can regulate A549 cell cycle progression in cisplatin-treated cells.

3.4. Retinoic acid affects cisplatin-induced apoptosis and cell autophagy

To evaluate the effects of RA pre-treatment on A549 cell resistance to cisplatin, we performed the following experiments. First, cell viability was assessed by the MTT assay. Combined treatment of cisplatin and RA at increasing concentrations reduced cell viability to a greater extent than these treatments alone (Fig. 4A). It is worth noting that no potentiation effects were observed in this assay, since the combined effect was not greater than the sum of each individual effect. Regarding the LDH activity assay, RA-treated cells showed no significant differences from the DMSO group (Fig. 4B control group), indicating no cytotoxic effects at this concentration, as previously observed (Fig. 1B). Meanwhile, cisplatin treatment at 10 μg/mL was able to increase LDH leakage by two-fold within 48 h. This increase was significantly higher in RA pre-treated cells (three-fold) than with DMSO pre-treatment (Fig. 4B cisplatin group). Considering that RA alone showed no effect compared to DMSO, but cisplatin alone showed a 100% increase and combination treatment (cisplatin + RA) showed a 200% increase, we postulated that RA potentiated the effect of cisplatin regarding the induction of cell death. To investigate the influence of thiol antioxidants defences, NAC (5 mM) was added to the cells 30 min before cisplatin. Interestingly, NAC treatment at this concentration had no significant effect on cisplatin-induced cell death (Fig. 4B cisplatin + NAC group vs. DMSO), but significantly protected against RA pre-treatment (Fig. 4B cisplatin + NAC group vs. RA).

The frequency of apoptotic/necrotic cells was quantified by annexin V/PI staining 24 h after cisplatin treatment. Representative populations are presented in Fig. 4C(II) and total apoptosis (early + late) results are shown in Fig. 4C(I). RA alone did not induce apoptosis in A549 cells. However, when combined with cisplatin treatment, it elevated the percentage of apoptotic cells to about 20% in comparison to 15% with cisplatin treatment alone (Fig. 4C). NAC co-incubation with cisplatin inhibited the RA pre-incubation effect (Fig. 4C), suggesting that the RA-

induced sensitivity of A549 cells is in fact correlated with the thiol antioxidants systems.

Finally, the induction of autophagy in A459 cells was evaluated in the presence of these treatments. RA alone increased the frequency of autophagy-positive cells by about 12% in comparison to DMSO (Fig. 4D). As expected, cisplatin alone increased the autophagic cell frequency in the population. Also, RA pre-treated cells given cisplatin showed a higher frequency of autophagy when compared to cisplatin alone at 24 h (Fig. 4D cisplatin vs. cisplatin + RA), but without a potentiation effect. Curiously, NAC co-incubation increased the number of autophagic cells by about 10% in both cisplatin- and cisplatin + RA-treated cells in comparison to the control (Fig. 4D).

4. Discussion

In the present study, RA treatment at pharmacological

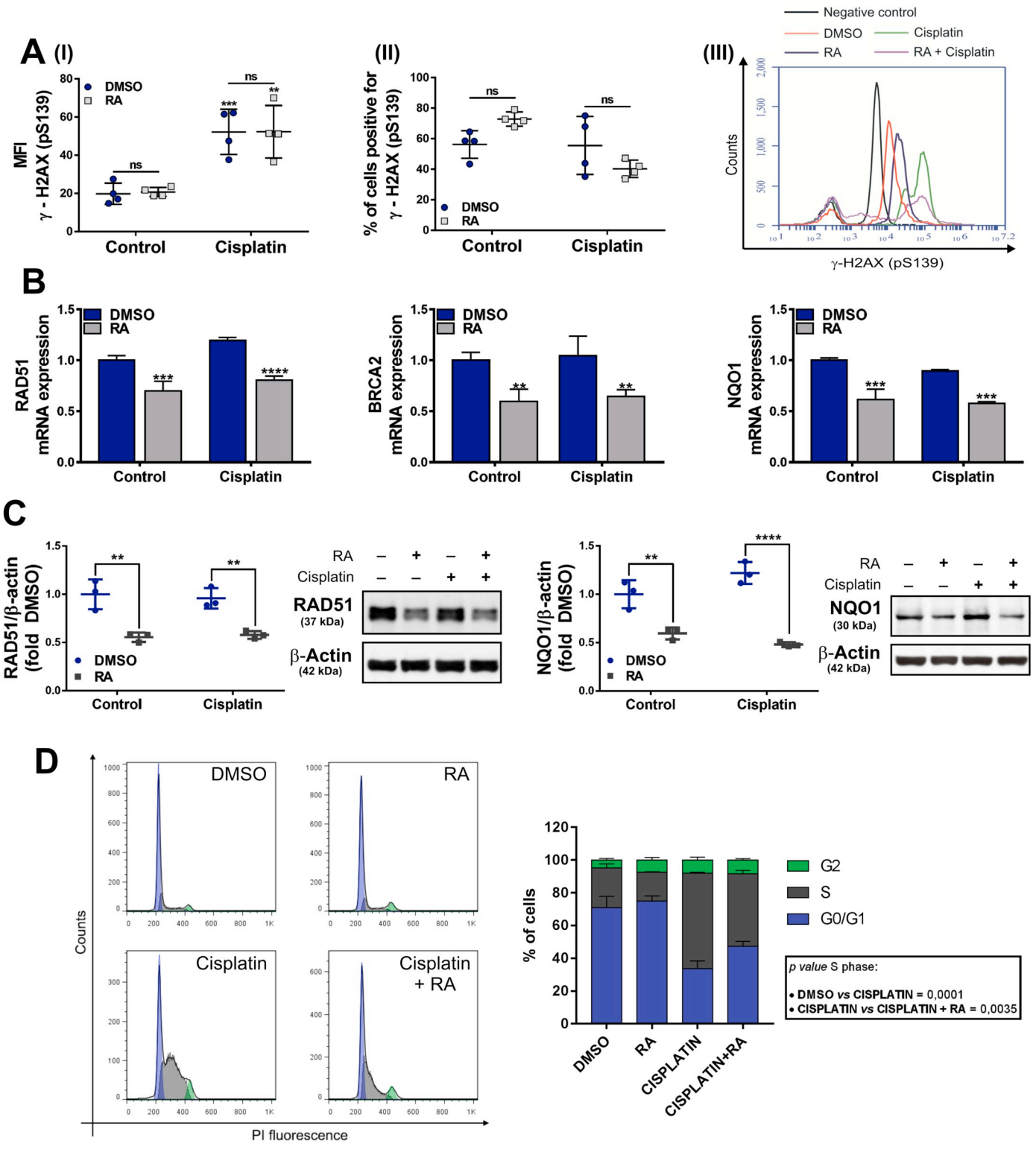

(caption on next page)

Fig. 3. Retinoic acid affects cisplatin-induced homologous recombination proteins expression, cell cycle arrest, but not phosphorylation of γ-*H2AX*. A549 cells were pre-treated for 48 h with RA 20 μM or DMSO before cisplatin (10 μg/mL) addition and the following analyzes were conducted. (A) Intracellular labeling of phosphorylated (pS139) γ-H2AX analysed by flow cytometry 16 h after cisplatin exposure. Graph **(I)** represents median fluorescence intensity (MFI), graph **(II)** represents the percentage of cells positively labelled for phospho- γ-H2AX and graph **(III)** is a representative overlay histogram of fluorescence intensity (x-axis) against counts of cell number (y-axis). Two-way ANOVA followed by Bonferroni post hoc test was conducted comparing groups. Graph A**(I)** asterisks are representing difference between control and cisplatin group within DMSO and RA groups. (B) mRNA levels of *RAD51*, *BRCA2* and *NQO1* genes measured by RT-qPCR. Results are expressed in mRNA fold-change relative to DMSO treatment at control group (no cisplatin). Relative quantification was obtained by $2 - \Delta\Delta CT$ method using GNB2L as housekeeping gene. Two-way ANOVA followed by Bonferroni post hoc test was conducted comparing RA treatment to DMSO treatment within control and cisplatin group. (C) Western blot analysis indicating RAD51 and NQO1 proteins immunocontent. Graphs show replicates quantification values and are expressed as fold-change relative to DMSO. Representative western blot image is shown on the right of each respective graph. β-Actin immunocontent is shown as loading control. Two-way ANOVA followed by Bonferroni post hoc test was conducted comparing RA treatment to DMSO treatment within control and cisplatin group. (D) Cell cycle was accessed by PI staining of permeabilized cells and measured by flow cytometry. Left image is representative of cytometer histogram showing cell number (y-axis) vs. PI fluorescence (x-axis). Right graph shows the relative percentage of cells in each cell cycle phase. Two-way ANOVA followed by Tukey's post hoc test was conducted to each cell cycle phase, comparing all means. Relevant *p* values of S phase are shown in the bottom-right corner board. Other relevant *p* values are described in the results section. Graphs are shown by means ± SD. *, **, *** and **** means $p < .05$, $p < .01$, $p < .001$ and $p < .0001$, respectively. NS means not significant.

concentrations presented inhibitory effects on A549 cell proliferation, NRF2 expression and activity (Section 3.1), as well as increased RS production, mitochondrial superoxide generation, concomitant with increased thiol group oxidation (Section 3.2). When combined with cisplatin treatment, RA was able to downregulate HR signalling proteins without changes in γ-H2AX phosphorylation, while interfering with cisplatin-induced cell cycle arrest (Section 3.3). Taken together, these effects correlated with increased efficacy in terms of triggering apoptosis with combined treatment (Section 3.4).

A549 cells responded to RA with significantly decreased proliferation and no lethal toxicity when exposed to pharmacological doses (10, 20, and 40 μM) (Fig. 1A and B). This antiproliferative effect agrees with previously published data in the literature [5]. Interestingly, NRF2 activity is correlated with cancer cell proliferation, since it regulates the expression of enzymes that redirect glucose metabolism to anabolic pathways such as the pentose phosphate pathway [12,30]. Accordingly, we observed the downregulation of *G6PD*, *TKT*, and *TALDO1* expression after RA treatment (Fig. 1D). The antiproliferative effects of RA have been mostly associated with the regulation of cell cycle proteins [31], but these data give a new perspective to investigate the correlation of NRF2 activity with RA antiproliferative properties.

Our results demonstrate that RA has an inhibitory effect on the NRF2 pathway in A549 cells. After 48 h, not only was the expression of NRF2 target genes downregulated, but also the NRF2 mRNA and protein content (Fig. 1D and E). This is of great significance because the initiation and progression of many lung cancers (including A549 cells) are associated with Keap-1 mutations [32] that allow NRF2 to translocate freely to the cell nucleus, increasing its promoter activity. NRF2 activity is also highly associated with cisplatin resistance in cancer cells [26]. Thus, downregulation of its gene expression is an important target for cancer prevention and therapy. Yet, this effect should be investigated in different models to confirm that is not cell line specific.

Regarding the involved signalling mechanisms, the fact that the *NQO1*, *GCLC*, and *GCLM* genes were downregulated after 24 h of RA treatment (Fig. 1D) leads us to think that other mechanisms are involved in NRF2 inhibition, not only through gene expression regulation. In fact, the reduced NRF2 content could be a consequence of previous inhibition of NRF2 promoter activity inside the nucleus, since this transcription factor is able to autoregulate its expression [33]. In line with this thought, it is known that RA can promote retinoic acid receptor alpha (RARα) interactions with NRF2 protein, inhibiting its activation in MCF-7 cells [17]. Also, retinoid X receptor alpha (RXRα) can act as NRF2 inhibitor through direct protein-protein interactions in A549 cells, even in the absence of ligands [34]. Therefore, more studies are necessary to investigate the role of RXR and RAR receptors on RA modulation of the NRF2 pathway. As a second hypothesis, we could consider that RA is not acting directly in the cell nucleus to downregulate NRF2 activity, but it could be rather selecting the proliferation of a subpopulation of cells with lower NRF2 expression, leading to a lower mRNA and protein content in the RT-qPCR and western blot experiments. Either way, RA treatment resulted in less NRF2 activity in A549 cells, indicating an advantageous perspective in the treatment of lung cancer.

In our results, we found that RA treatment increased RS production in A549 cells during the initial hours of exposure (Fig. 2A and B). This increase was correlated with the generation of mitochondrial superoxide (Fig. 2C), indicating that mitochondria can be affected by RA in this model. Importantly, protein thiol groups within mitochondria are one of the first targets of cisplatin-induced oxidative stress [26]. Even though an increased production rate of RS was decreased after 6 h, a higher concentration of oxidised thiol groups was observed in RA-treated cells after 24 and 48 h (Fig. 2D), indicating a pro-oxidant cellular environment. Thioredoxin enzymes are responsible for restoring oxidised thiol groups of proteins after oxidative damage, depending on reduced glutathione (GSH) as a substrate [35]. In our results, glutathione synthesis is likely compromised after 24 h since the expression of *GCLC* and *GCLM* genes are downregulated, compromising antioxidant defences. After 48 h, not only was glutathione synthesis downregulated, but the *TXNRD1* gene, responsible for the regeneration of thioredoxin activity, was also downregulated, likely compromising the repair of oxidative damage to thiol groups within proteins. It is worth noting that many of thiol antioxidant defence enzymes are dependent on NADPH molecules, especially to restore GSH levels [36]. Genes associated with NADPH generation (*G6PD* and *ME1*) were also downregulated after 48 h of RA treatment, jeopardising antioxidant defences. Even though more studies are necessary to establish a clear association between RA pro-oxidant activity during the initial hours and NRF2 downregulation at 24 and 48 h, as a final result we observed a clear downregulation of many thiol antioxidant enzymes and a more oxidative environment within the cell, caused by RA treatment after 48 h (Fig. 2D). Cancer cells are highly dependent on antioxidant defences since they usually have a higher concentration of RS than normal cells [37]. Therefore, inhibiting such pathways can selectively lead to oxidative stress in cancer cells rather than normal cells, even without a pro-oxidant agent [37]. Likewise, oxidative stress is known to be a fundamental pathway responsible for cisplatin cytotoxicity; glutathione defences are responsible for cell resistance [26], corroborating that RA pre-treatment impairs important resistance mechanisms to cisplatin in A549 cells. Taken together with the fact that NAC co-treatment totally reversed the RA potentiation effect regarding cisplatin-induced cell death (Fig. 4B and C), it becomes clear that thiol antioxidant defences associated with NRF2 activity are an important pathway through which RA pre-treatment sensitises A549 cells to cisplatin cytotoxicity. In agreement, it has been demonstrated that NRF2 inhibition through siRNA potentiates cisplatin cytotoxicity in A549 cells [10]. One concern regarding lung cancer patient treatment would be that RA could also increase cytotoxicity in normal cells. However, clinical trials that have tested RA in combination with cisplatin and paclitaxel did not observe

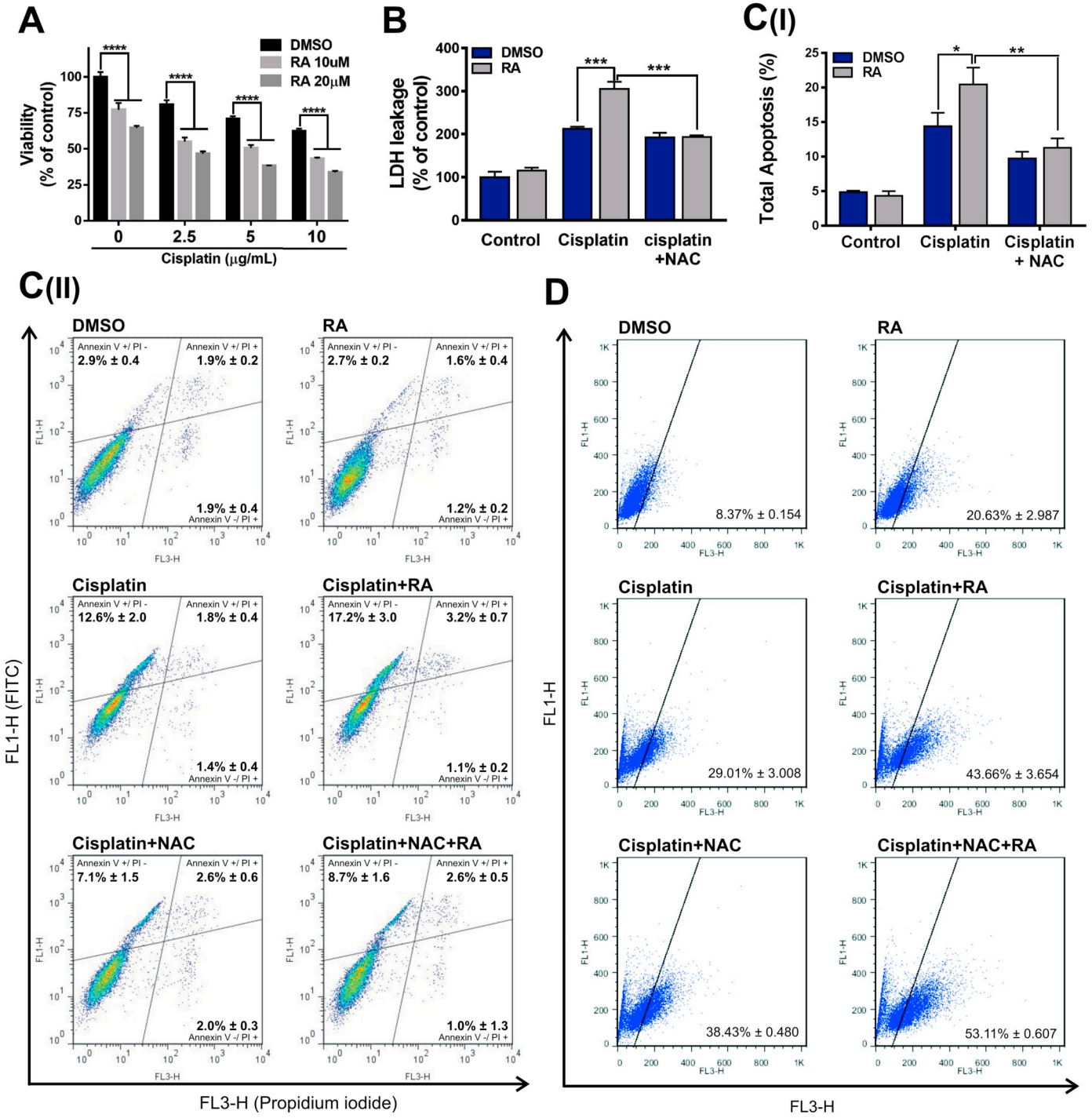

Fig. 4. Retinoic affects cisplatin-induced apoptosis and cell autophagy. A549 cells were pre-treated with RA for 48 h when cisplatin was added to the cells and incubated. At the end, the following experiments were conducted. (A) Cell viability was measured by MTT assay after cells pre-treatment with 10 and 20 μM of RA followed by 0, 2.5, 5 and 10 μg/mL of cisplatin exposure for 48 h. Results are expressed as percentage of experiment control (DMSO treatment without cisplatin). Two-way ANOVA followed by Bonferroni post hoc test was conducted comparing RA treatments to DMSO within each cisplatin concentration. (B) The percentage of dead cells measured by LDH activity in culture medium (LDH leakage) after 20 μM of RA pre-treatment followed by 10 μg/mL of cisplatin exposure for 48 h. In the Cisplatin + NAC group, *N*-acetyl cysteine (5 mM) was added to the cells 30 min before cisplatin and the experiment was conducted as usual. Results are expressed as percentage of experiment control (DMSO treatment without cisplatin). Two-way ANOVA followed by Tukey's post hoc test was conducted to evaluate statistical significance. (C) Frequency of apoptotic cells measured by annexin V – FITC/ PI staining and quantified by flow cytometry. A549 cells were pre-treated with 20 μM of RA followed by 10 μg/mL of cisplatin exposure for 24 h. In the Cisplatin + NAC group, *N*-acetyl cysteine (5 mM) was added to the cells 30 min before cisplatin and the experiment was conducted as usual. C**(I)** graph indicates the percentage of total apoptosis (early + late). Results are expressed as percentage of experiment control (DMSO treatment without cisplatin). Two-way ANOVA followed by Tukey's post hoc test was conducted to evaluate statistical significance. C**(II)** figures are representative of cells population observed in the cytometer. *Y*-axis indicates Annexin V-FITC fluorescence and *x*-axis indicates PI fluorescence. Gates titles and frequency means ± SD are indicated in each fig. (D) Indicative of autophagic activity measured by acridine orange red fluorescence quantified by flow cytometry. A549 cells were pre-treated with 20 μM of RA followed by 10 μg/mL of cisplatin exposure for 24 h. In the Cisplatin + NAC group, *N*-acetyl cysteine (5 mM) was added to the cells 30 min before cisplatin and the experiment was conducted as usual. Two-way ANOVA followed by Tukey's post hoc test was conducted to evaluate statistical significance. Figures are representative of cells population observed in the cytometer. *Y*-axis indicates FL1-H channel fluorescence and *x*-axis indicates FL3-H channel fluorescence. Frequency means ± SD are indicated in each figure. Graphs are shown by means ± SD. *, **, *** and **** means $p < .05$, $p < .01$, $p < .001$ and $p < .0001$, respectively. (For interpretation of the references to colour in this figure legend, the reader is referred to the web version of this article.)

increased toxicity in patients; rather, RA was able to reduce neuropathy induced by chemotherapy [6,7].

Along with oxidative stress, inter-strand DNA cross-links that leads to double-strand break (BSB) damage is a fundamental mechanism of cisplatin cytotoxicity [26]. Homologous recombination is the most important and effective pathway activated in tumour cells to perform double-strand break repair [27]. Here, we have demonstrated that RA pre-treatment downregulated RAD51 and BRCA2 expression in A549 cells (Fig. 3). Simultaneously, it also decreased NQO1 gene expression and protein content, which is an indicative of NRF2 activity. NRF2 protein was shown to promote the expression of DNA repair-related proteins, including the expression of RAD51 in A549 cells exposed to radiation [14,38]. Thus, it is proposable that suppressed HR is linked to NRF2 inhibition in RA pre-treated cells.

Even though decreased expression and immunocontent of HR proteins was observed, RA pre-treatment did not sensitise A549 cells to cisplatin-mediated induction of phospho-γ-H2AX, as shown by the MFI results (Fig. 3A-I). It is expected that the downregulation of HR proteins leads to the persistence of DNA damage and therefore an accumulation of phosphor-γ-H2AX foci [39]. Therefore, our results indicate that HR protein downregulation is not sufficient to impair the DNA damage response in A549 cells treated with cisplatin, at least at our experimental conditions. Other mechanisms may be responsible for DSB repair, such as non-homologous end joining (NHEJ), and therefore be effective in this context. In fact, HR is a process virtually exclusive to cells in the late S-phase and G2-phase due to the necessity for sister chromatids for correct function [29,38]. Thus, the effect of RA on decreasing the percentage of S-phase cells after cisplatin treatment probably contributed to HR suppression, favouring other DNA repair pathways. Nevertheless, many results in the literature support the notion that RAD51 expression is highly associated with cisplatin-resistant cells [27,28], while other strategies targeting RAD51 with siRNA or gefitinib (an epidermal growth factor receptor (EGFR) inhibitor) were able to increase the sensitivity of A549 cells to cisplatin (reviewed by [27]).

Autophagic process are known to be activated in response to different stressors, and are able to promote both cell death and survival [40]. In line with this observation, the autophagic cell population was increased by cisplatin treatment alone. RA alone increased AO red fluorescence (Fig. 4D), suggesting autophagosome activation. These results agree with other authors in that autophagy is a required mechanism for RA-mediated cell differentiation [41] and counteracts the pro-apoptotic effects in breast cancer cells [42]. Furthermore, the cisplatin + RA group presented a higher percentage of autophagy than the individual groups. However, this effect was not additive since the percentage value (43%) was inferior to the sum of both individually (49%). It is possible that RA potentiation of cisplatin pro-apoptotic effects causes cells to overcome the autophagic process and trigger apoptosis instead. In fact, we observed an increase of 5% in apoptotic cells with combination treatment, which is similar to the 6% of the population that were not positive for autophagy, as expected for an additive effect. Nevertheless, the relation between apoptosis and autophagy is still a complex subject and further studies are necessary to better understand whether autophagy is acting as a resistance mechanism or contributing to apoptotic fate.

Interestingly, RS can trigger protective autophagy in cancer cells. This process is associated with activation of p62 protein, which recruits oxidised proteins to autophagosomes for degradation. The NRF2 pathway has been shown to promote p62 expression, creating crosstalk between antioxidant defences and protective autophagy, and counteracting oxidative damage (revised by [37]). Thus, the downregulation of NRF2 and the antioxidant systems by RA could be suppressing autophagic efficiency and simultaneously leading to RS accumulation after cisplatin exposure, promoting the activation of apoptotic pathways [37]. This observation agrees with the fact that NAC incubation suppressed apoptosis and promoted autophagy, likely by regulating RS levels and compensating for thiol antioxidant system downregulation.

5. Conclusion

It is known that cisplatin cytotoxicity is associated with two major mechanisms: oxidative stress and DNA cross-links [26]. Also, cancer cells become resistant to cisplatin treatment, usually by upregulating antioxidant systems [37,43] and DNA repair pathways [27]. Hence, the fact that RA suppresses NRF2, the thiol antioxidant system, and homologous recombination signalling proteins in A549 cells supports its administration in combination with cisplatin chemotherapy. Downregulation of RAD51 by other strategies was shown to improve cisplatin effects in lung cancer cells, however this was not clear in our results. The effects of RA on the cell cycle progression and its influence on DNA repair pathways may be a focus of study on this regard. Moreover, elevated NRF2 activity is highly correlated with poor prognosis in lung cancer, making RA an important effector in this context. Nevertheless, we understand that this work has important limitations, specially that the results are limited to the A549 cell model.

Importantly, this work contributes to recent literature showing that a combination of RS generating chemicals allied to antioxidant system inhibitors might be a promising strategy in cancer treatment [37,43], corroborating the necessity to further investigate such mechanisms in the combination of RA with other chemotherapies. Lastly, the use of a pharmacological inhibitor targeting autophagic pathways is an urgent necessity to better understand the role of autophagy in this context.

Acknowledgments

We acknowledge the Brazilian funds CAPES, FAPERGS/CNPq – PRONEX 16/2551-0000 499-4 and, FAPERGS/MS/CNPq/SESRS - PPSUS 17/2551-0001 408-1 and PPG-Bioquímica/UFRGS.

Declaration of interest

None.

References

[1] G. Duester, Retinoic acid synthesis and signaling during early organogenesis, Cell 134 (2008) 921–931.
[2] S. Nagpal, Retinoids: inducers of tumor/growth suppressors, J. Invest. Dermatol. 123 (2004) 1–2.
[3] L.I.N. Shi, H. Li, Y. Zhan, All - trans retinoic acid enhances temozolomide - induced autophagy in human glioma cells U251 via targeting Keap1/Nrf2/ARE signaling pathway, Oncol. Lett. (2017) 2709–2714.
[4] Y. Zhang, D.X. Guan, J. Shi, H. Gao, J.J. Li, J.S. Zhao, L. Qiu, J. Liu, N. Li, W.X. Guo, J. Xue, F.G. Zhou, M.C. Wu, H.Y. Wang, D. Xie, S.Q. Cheng, All-trans retinoic acid potentiates the chemotherapeutic effect of cisplatin by inducing differentiation of tumor initiating cells in liver cancer, J. Hepatol. 59 (6) (2013) 1255–1263.
[5] B. Li, M.-H. Gao, X.-M. Chu, L. Teng, C.-Y. Lv, P. Yang, Q.-F. Yin, The synergistic antitumor effects of all-trans retinoic acid and C-phycocyanin on the lung cancer A549 cells in vitro and in vivo, Eur. J. Pharmacol. 749 (2015) 107–114.
[6] O. Arrieta, C.H. González-De La, E. Rosa, G. Aréchaga-Ocampo, T.L. Villanueva-Rodríguez, L. Cerón-Lizárraga, M.E. Martínez-Barrera, M.Á. Vázquez-Manríquez, M.Á. Ríos-Trejo, N. Álvarez-Avitia, C. Rojas-Marín Hernández-Pedro, J. De La Garza, Randomized phase II trial of all-trans-retinoic acid with chemotherapy based on paclitaxel and cisplatin as first-line treatment in patients with advanced non-small-cell lung cancer, J. Clin. Oncol. 28 (21) (2010) 3463–3471.
[7] O. Arrieta, N. Hernandez-Pedro, M.C. Fernandez-Gonzalez-Aragon, D. Saavedra-Perez, A.D. Campos-Parra, M.A. Rios-Trejo, T. Ceron-Lizarraga, L. Martinez-Barrera, B. Pineda, G. Ordonez, A. Ortiz-Plata, V. Granados-Soto, J. Sotelo, Retinoic acid reduces chemotherapy-induced neuropathy in an animal model and patients with lung cancer, Neurology 77 (10) (2011) 987–995.
[8] R.M. Connolly, N.K. Nguyen, S. Sukumar, Molecular pathways: current role and future directions of the retinoic acid pathway in cancer prevention and treatment, Clin. Cancer Res. 19 (7) (2013) 1651–1959.
[9] T. Schenk, S. Stengel, A. Zelent, Unlocking the potential of retinoic acid in anticancer therapy, Br. J. Cancer 111 (11) (2014) 2039–2045.
[10] S. Homma, Y. Ishii, Y. Morishima, T. Yamadori, Y. Matsuno, N. Haraguchi, N. Kikuchi, H. Satoh, T. Sakamoto, N. Hizawa, K. Itoh, M. Yamamoto, Nrf2 enhances cell proliferation and resistance to anticancer drugs in human lung cancer, Clin. Cancer Res. 15 (10) (2009) 3423–3432.
[11] G.M. DeNicola, F.A. Karreth, T.J. Humpton, A. Gopinathan, C. Wei, K. Frese,

D. Mangal, K.H. Yu, C.J. Yeo, E.S. Calhoun, F. Scrimieri, J.M. Winter, R.H. Hruban, C. Iacobuzio-donahue, S.E. Kern, I.A. Blair, D.A. Tuveson, Oncogene-induced Nrf2 transcription promotes ROS detoxification and tumorigenesis, Nature 475 (7354) (2011) 106–109.
[12] Y. Mitsuishi, K. Taguchi, Y. Kawatani, T. Shibata, T. Nukiwa, H. Aburatani, M. Yamamoto, H. Motohashi, Nrf2 redirects glucose and glutamine into anabolic pathways in metabolic reprogramming, Cancer Cell 22 (1) (2012) 66–79.
[13] I.I.C. Chio, S.M. Jafarnejad, M. Ponz-Sarvise, Y. Park, K. Rivera, W. Palm, J. Wilson, V. Sangar, Y. Hao, D. Öhlund, K. Wright, D. Filippini, E.J. Lee, B. Da Silva, C. Schoepfer, J.E. Wilkinson, J.M. Buscaglia, G.M. DeNicola, H. Tiriac, M. Hammell, H.C. Crawford, E.E. Schmidt, C.B. Thompson, D.J. Pappin, N. Sonenberg, D.A. Tuveson, NRF2 promotes tumor maintenance by modulating mRNA translation in pancreatic cancer, Cell 166 (4) (2016) 963–976.
[14] S. Jayakumar, D. Pal, S.K. Sandur, Nrf2 facilitates repair of radiation induced DNA damage through homologous recombination repair pathway in a ROS independent manner in cancer cells, Mutat. Res. Fundam. Mol. Mech. Mutagen. 779 (2015) 33–45.
[15] M. Pajares, N. Jiménez-Moreno, Á.J. García-Yagüe, M. Escoll, M.L. de Ceballos, F. Van Leuven, A. Rábano, M. Yamamoto, A.I. Rojo, A. Cuadrado, Transcription factor NFE2L2/NRF2 is a regulator of macroautophagy genes, Autophagy 12 (10) (2016) 1902–1916.
[16] L. Baird, D. Llères, S. Swift, A.T. Dinkova-kostova, Regulatory fl exibility in the Nrf2-mediated stress response is conferred by conformational cycling of the Keap1-Nrf2 protein complex, PNAS 110 (38) (2013) 15259–15264.
[17] X.J. Wang, J.D. Hayes, C.J. Henderson, C.R. Wolf, Identification of retinoic acid as an inhibitor of transcription factor Nrf2 through activation of retinoic acid receptor alpha, Proc. Natl. Acad. Sci. U. S. A. 104 (49) (2007) 19589–19594.
[18] F. Zhao, T. Wu, A. Lau, T. Jiang, Z. Huang, X.-J. Wang, W. Chen, P.K. Wong, D.D. Zhang, Nrf2 promotes neuronal cell differentiation, Free Radic. Biol. Med. 47 (6) (Sep. 2009) 867–879.
[19] P. Skehan, R. Storeng, D. Scudiero, J. Monks, D. McMahon, J.T. Vistica, H. Warren, S. Kenney Bokesch, M.R. Boyd, New colorimetric cytotoxicity assay for anticancer-drug screening, J. Natl. Cancer Inst. 82 (1990) 1107–1112.
[20] V. de Miranda Ramos, A. Zanotto-Filho, M.A. de Bittencourt Pasquali, K. Klafke, J. Gasparotto, P. Dunkley, D.P. Gelain, J.C.F. Moreira, NRF2 mediates neuroblastoma proliferation and resistance to retinoic acid cytotoxicity in a model of in vitro neuronal differentiation, Mol. Neurobiol. 53 (9) (2016) 6124–6135.
[21] H. Wang, J. Joseph, Quantifying cellular oxidative stress by dichlorofluorescein assay using microplate reader, Free Radic. Biol. Med. 27 (99) (1999) 612–616.
[22] G.L. Ellman, Tissue sulfhydryl groups, Arch. Biochem. abd Biophys. 82 (1959) 70–77.
[23] M.P. Thomé, E.C. Filippi-Chiela, E.S. Villodre, C.B. Migliavaca, G.R. Onzi, K.B. Felipe, G. Lenz, Ratiometric analysis of acridine orange staining in the study of acidic organelles and autophagy, J. Cell Sci. 129 (24) (2016) 4622–4632.
[24] A. Zanotto-Filho, M. Cammarota, D.P. Gelain, R.B. Oliveira, A. Delgado-Cañedo, R.J.S. Dalmolin, M. a B. Pasquali, J.C.F. Moreira, Retinoic acid induces apoptosis by a non-classical mechanism of ERK1/2 activation, Toxicol. in Vitro 22 (2008) 1205–1212.
[25] N.K. Zenkov, E.B. Menshchikova, V.O. Tkachev, Keap1/Nrf2/ARE redox-sensitive signaling system as a pharmacological target, Biokhimiya/Biochemistry 78 (1) (2013) 19–36.
[26] D. Shaloam, P.B. Tchounwou, Cisplatin in cancer therapy: molecular mechanisms of action, Eur. J. Pharmacol. 740 (2014) 364–378.
[27] S. O'Grady, S.P. Finn, S. Cuffe, D.J. Richard, K.J. O'Byrne, M.P. Barr, The role of DNA repair pathways in cisplatin resistant lung cancer, Cancer Treat. Rev. 40 (10) (2014) 1161–1170.
[28] S. Adam-Zahir, P.N. Plowman, E.C. Bourton, F. Sharif, C.N. Parris, Increased γ-H2AX and Rad51 DNA repair biomarker expression in human cell lines resistant to the chemotherapeutic agents nitrogen mustard and cisplatin, Chemotherapy 60 (5–6) (2015) 310–320.
[29] D. Branzei, M. Foiani, Regulation of DNA repair throughout the cell cycle, Nat. Rev. Mol. Cell Biol. 9 (4) (2008) 297–308.
[30] J.D. Hayes, M.L.J. Ashford, Nrf2 orchestrates fuel partitioning for cell proliferation, Cell Metab. 16 (2012) 139–141.
[31] X.-H. Tang, L.J. Gudas, Retinoids, retinoic acid receptors, and cancer, Annu. Rev. Pathol. 6 (2011) 345–364.
[32] A. Lau, N.F. Villeneuve, Z. Sun, P.K. Wong, D.D. Zhang, Dual roles of Nrf2 in cancer, Pharmacol. Res. 58 (2008) 262–270.
[33] J.D. Hayes, A.T. Dinkova-Kostova, The Nrf2 regulatory network provides an interface between redox and intermediary metabolism, Trends Biochem. Sci. 39 (4) (2014) 199–218.
[34] H. Wang, K. Liu, M. Geng, P. Gao, X. Wu, Y. Hai, Y. Li, Y. Li, L. Luo, J.D. Hayes, X.J. Wang, X. Tang, RXRα inhibits the NRF2-ARE signaling pathway through a direct interaction with the Neh7 domain of NRF2, Cancer Res. 73 (10) (2013) 3097–3108.
[35] A. Matsuzawa, Thioredoxin and redox signaling: roles of the thioredoxin system in control of cell fate, Arch. Biochem. Biophys. 617 (2017) 101–105.
[36] M.D. Shelly, C. Lu, Glutathione synthesis, Biochim. Biophys. Acta 1830 (5) (2014) 3143–3153.
[37] S. Galadari, A. Rahman, S. Pallichankandy, F. Thayyullathil, Reactive oxygen species and cancer paradox: to promote or to suppress? Free Radic. Biol. Med. 104 (2017) 144–164 no. August 2016.
[38] K.R. Sekhar, M.L. Freeman, Nrf2 promotes survival following exposure to ionizing radiation, Free Radic. Biol. Med. 88 (2015) 268–274 Part B.
[39] P.L. Olive, J.P. Banàth, Kinetics of H2AX phosphorylation after exposure to cisplatin, Cytom. Part B - Clin. Cytom. 76 (2) (2009) 79–90.
[40] S. Fulda, A.M. Gorman, O. Hori, A. Samali, Cellular stress responses: cell survival and cell death, Int. J. Cell Biol. 2010 (2010).
[41] N. Orfali, T.R. O'Donovan, M.J. Nyhan, A. Britschgi, M.P. Tschan, M.R. Cahill, N.P. Mongan, L.J. Gudas, S.L. McKenna, Induction of autophagy is a key component of all-trans-retinoic acid-induced differentiation in leukemia cells and a potential target for pharmacologic modulation, Exp. Hematol. 43 (9) (2015) 781–793.
[42] D. Brigger, A.M. Schläfli, E. Garattini, M.P. Tschan, Activation of RARα induces autophagy in SKBR3 breast cancer cells and depletion of key autophagy genes enhances ATRA toxicity, Cell Death Dis. 6 (8) (2015) 1–10.
[43] A. Bansal, M. Celeste Simon, Glutathione metabolism in cancer progression and treatment resistance, J. Cell Biol. 217 (7) (2018) 2291–2298.